

Mapping the suitability for ice-core drilling of glaciers in the European Alps and the Asian High Mountains

ROBERTO GARZONIO,¹ BIAGIO DI MAURO,¹ DANIELE STRIGARO,²
MICOL ROSSINI,¹ ROBERTO COLOMBO,¹ MATTIA DE AMICIS,¹ VALTER MAGGI¹

¹Department of Earth and Environmental Sciences, University of Milano-Bicocca, Italy

²Department for Environment Constructions and Design, Institute of Earth Sciences, University of Applied Sciences and Arts of Southern Switzerland, Canobbio, Switzerland

Correspondence: Roberto Garzonio <roberto.garzonio@unimib.it>

ABSTRACT. Ice cores from mid-latitude mountain glaciers provide detailed information on past climate conditions and regional environmental changes, which is essential for placing current climate change into a longer term perspective. In this context, it is important to define guidelines and create dedicated maps to identify suitable areas for future ice-core drillings. In this study, the suitability for ice-core drilling (SICD) of a mountain glacier is defined as the possibility of extracting an ice core with preserved stratigraphy suitable for reconstructing past climate. Morphometric and climatic variables related to SICD are selected through literature review and characterization of previously drilled sites. A quantitative Weight of Evidence method is proposed to combine selected variables (i.e. slope, local relief, temperature and direct solar radiation) to map the potential drilling sites in mid-latitude mountain glaciers. The method was first developed in the European Alps and then applied to the Asian High Mountains. Model performances and limitations are discussed and first indications of new potential drilling sites in the Asian High Mountains are provided. Results presented here can facilitate the selection of future drilling sites especially on unexplored Asian mountain glaciers towards the understanding of climate and environmental changes.

KEYWORDS: glacial geomorphology, glacier modelling, ice core, mountain glaciers

Abbreviations: SICD: suitability for ice-core drilling, WoE: Weight of Evidence, IDB: Ice-core DataBase, RGI: Randolph Glacier Inventory, CDF: cumulative distribution functions, DEM: Digital Elevation Model, GIS: Geographic Information System, GRASS: Geographic Resources Analysis Support System, RMSE: root-mean-square error, AUC: area under the curve, ASTER: Advanced Spaceborne Thermal Emission and Reflection Radiometer, NAO: North Atlantic Oscillation, ENSO: El Niño–Southern Oscillation

1. INTRODUCTION

Ice cores are excellent archives for documenting paleoclimatic conditions and for gaining a better understanding of recent climatic and environmental variability affecting wide regions of the Earth (Delmas, 1992; Alley, 2000). Polar ice cores, such as those extracted from Greenland and Antarctica, allow to reconstruct glacial and interglacial cycles through global or hemispheric signals of past temperature, precipitation, aerosol concentration, greenhouse gases and so on (Andersen and others, 2004; Epica, 2004, 2006; Kawamura and others, 2007; Orombelli and others, 2010; Faria and others, 2014). However, polar ice cores have limited value for studying local climatic variability because they are far from low- and mid-latitude regions where most of the Earth's population lives.

On the other hand, ice cores recovered from mid-latitude mountain glaciers offer excellent archives for understanding recent climatic variability due to both natural and anthropogenic factors. Such ice cores present several advantages for studying climate changes (Thompson, 1996, 2010; Schwikowski and others, 1999; Vimeux and others, 2009; Thompson and others, 2011, 2013). First, mountain ice cores provide the opportunity to investigate the dynamics of atmospheric short-lived species emitted from populated

and industrialized areas often surrounding mountain glaciers (Döschner and others, 1995; Preunkert and others, 2000; Schuster and others, 2002; Schwikowski and others, 2004; Buffen and others, 2014). Secondly, long-term, high-quality instrumental records are often available in the proximity of mountain glaciers. This allows a detailed characterization of the transfer processes and the deposition rates of various atmospheric constituents through the comparison between direct measurements and ice-core data (Schotterer and others, 1997; Tian and others, 2003; Mariani and others, 2014). Furthermore, mid-latitude areas are generally characterized by high precipitation rates allowing the creation of records with higher temporal resolution (Thompson and others, 2003, 2005; Kaspari and others, 2007; Neff and others, 2012) than the ones extracted from ice sheets (Petit and others, 1999; Svensson and others, 2008; Jouzel and Masson-Delmotte, 2010). Finally, mountain ice cores allow the analysis of specific meteorological processes, as the Saharan dust depositions in the Alps (Jenk and others, 2006; Thevenon and others, 2009) and Himalaya (Kaspari and others, 2009a, b) or the intensity fluctuations of the South Asian Monsoon in the Tibetan Plateau (Thompson and others, 2000; Davis and Thompson, 2005).

In addition, as a result of recent global warming, low- and mid-latitude glaciers are retreating with an increased trend in recent years (Lowell, 2000; Beniston, 2005; Vincent and others, 2005; Bolch and others, 2012). Glacier melting could lead to a dramatic loss of important paleoclimatic records (Thompson, 2000; Zhang and others, 2015). For this reason, it is necessary to identify new areas of mountain glaciers where to collect new ice cores in the next years.

A fundamental contribution in the reconstruction and interpretation of environmental changes can arise from the selection of new potential drilling sites primarily located in unexploited mountain ranges. Among those, the Asian High Mountains are a very interesting region. Asia, in fact, is mainly affected by two regional weather systems (the west-lies and the Indian monsoon) and Asian glaciers are located adjacent to densely inhabited regions and their emerging economies. It is well known that ice cores from Asian mountains (e.g. Himalaya, Tibetan Plateau, Karakoram, Tien Shan) can provide useful data for understanding variability of both regional and global circulation (Aizen and others, 2006; Yang and others, 2014; Du and others, 2016) as well as the effect of anthropogenic activities on natural conditions (Zhao and others, 2011; Grigholm and others, 2016). The importance of the Asian High Mountains is also motivated by the fact that a large number of potential unexplored drilling sites are present in these remote areas and could be exploited.

One common feature of mountain ranges is the complexity of their topography and atmospheric dynamics. Atmospheric conditions (e.g. precipitation, temperature) and glacier topography (e.g. elevation, slope, aspect) play a key role in defining the location of an ice-core drilling site. Selecting an area suitable for ice-core drilling can therefore be challenging, especially in remote areas where little information is available. Some authors have investigated the relation between the quality of the stratigraphy and the glacier's features (Wagenbach and Geis, 1989; Welch and others, 1998; Campbell and others, 2012). This specific issue is typically examined for a glacier site based on ground explorations (Copland and Sharp, 2001; Schwikowski and others, 2006; Gabrielli and others, 2010). Traditional methods are impossible to perform at large scale for mapping potential drilling sites in remote areas such as the Asian High Mountains. However, gathering site-specific geophysical information at any specific site is critical both for identifying the best drill site and for interpretation of the ice-core records. In this context, the criteria governing the choice of a drilling site and the environmental factors that affect the possibility to drill a mountain glacier are poorly formalized in the available scientific literature. Accordingly, the development of a methodology to map potential sites, using simple, globally and spatially distributed variables, is relevant for the identification of new drilling sites.

The goal of this study is to develop a novel methodology to identify suitable areas for non-polar ice-core drilling that can be applied in unexplored areas for a preliminary identification of potential drilling sites. For this purpose, we first identify the morphometric and climatic variables associated to glacier suitability for ice-core drilling (SICD) based on the characteristics of already drilled sites in Alpine and Asian High Mountain glaciers. Then, we develop a statistical approach to map the SICD for these areas. Assuming that in the European Alps all available drilling sites have been already exploited, we use this area to create and evaluate

the model. Finally, we apply the model in the Asian High Mountains, and several new drilling sites are proposed and discussed providing important constraints in this poorly explored area.

2. REVIEW OF SICD

When snow accumulates on the glacier surface, the climatic signal is stored in the ice. Glaciers preserve, in each layer, differences in the chemistry and structure of ice, related to climatic and environmental conditions at the time of snow depositions. The morphological and physical features of the site (e.g. slope, glacier dynamics, flow velocity, ice thickness, melting), as well as the climatic variables (e.g. snow accumulation rate, wind exposure, temperature), determine snow and firn metamorphism, thus influencing the quality of the stratigraphy. For example, insolation and temperature gradients produce snow melting, recrystallization and densification, while the ice flow can mix the layers causing stratigraphic disturbance (Thompson, 2000; Schotterer and others, 2004; Cuffey and Paterson, 2010; Faria and others, 2010). In addition, surface processes such as drifting and selective removal or accumulation by wind (Faria and others, 2009; Birnbaum and others, 2010) can modify seasonal depositions of snow crystals, dust, aerosol and trace compounds.

Wagenbach and Geis (1989) summarized the glacio-meteorological and topographical criteria leaning towards the preservation of ice-core stratigraphy as follows: (i) high elevation, corresponding to low temperatures, to prevent water percolation; (ii) sufficient glacier thickness and reasonable snow accumulation rate to ensure long-term records and temporal resolution; (iii) large extension and relatively flat surface topography to minimize the influence of glacier flow. However, a physical model able to support the definition of new drilling areas is not available, whereas a series of ground exploration techniques (e.g. meltwater percolation studies, mass-balance reconstructions, geophysical thickness investigations, ice flow models, glacio-chemical analyses) are generally applied to individual glaciers to evaluate their SICD (Preunkert and others, 2000; Schwikowski and others, 2006; Campbell and others, 2012; Wagenbach and others, 2012).

The most important requirement when selecting a drilling site is the quality of the glacio-chemical signal stored in the ice. Table 1 summarizes the most relevant climatic and environmental variables affecting the quality of the glacio-chemical stratigraphy that should be considered in the selection of a new drilling site.

Another important criterion is the temporal resolution of the stratigraphy. It depends on the accumulation and distribution of snow precipitations and glacier thickness. An ice core can cover a long time span reaching back thousands of years or fewer decades with a high sub-seasonal detail. Generally, higher annual accumulation is associated with high resolved seasonal stratigraphy, while low accumulation rates preserve ice cores with a long time history. Seasonal signals can be useful for evaluating inter-annual variability (e.g. warmer summers, precipitation and extreme events, dust depositions, etc.) and calibrating climatic models (e.g. integration of climatic records with weather stations).

In the selection of a drilling site, its climatic relevance can be evaluated according to the research focus (e.g. relevance of the geographic location with respect to the investigated

Table 1. Variables that affect the preservation of the ice-core stratigraphy

Variables	Influence on the quality of stratigraphic preservation
Temperature and solar radiation	Suitable sites are located at high altitudes in shaded areas where surface temperatures remain generally below freezing point (particularly during summertime). These areas preserve the original stratigraphy from melting and percolation processes
Wind transport and avalanche mixing	The stratigraphy is altered by snow redistribution and mixing process caused by wind and avalanches. Suitable areas are characterized by low wind exposure (and deposition) and not impacted by avalanches
Glacier dynamics and ice flow	Glacier dynamics and ice flow can wrap and mix the layers, complicating the reading of the stratigraphy. Ice flow is associated with steepest slope gradients. Suitable sites are placed mainly in flat areas near ice divides characterized by low ice flows

processes). Individual glaciers, in fact, can store specific information as a function of their location; and the proximity of important sources (e.g. city, desert, volcano) can strongly influence other signals stored in the glacier.

All these requirements are difficult to formalize and many parameters are nearly impossible to obtain spatially distributed at the global scale. We chose to focus the proposed model only on the quality of the stratigraphy because of its importance in determining the potential of a drilling site. The rationale of this study is to combine a limited subset of relevant variables, identified through literature research, to propose a SICD index able to map the potential drilling sites of non-polar mountain glaciers.

3. DATA COLLECTION AND METHODOLOGY

In this study, we focused on non-polar mountain glaciers in the European Alps and in the Asian High Mountains due to the abundance of already drilled sites. The overall study area is shown in Figure 1. The European Alps are a complex mountain system that extends ~1000 km (from East to West) throughout south-central Europe, reaching a maximum elevation of 4800 m (at the Mont Blanc summit). The Alps are affected by different climatological regimes and can be divided into three geographical regions with different characteristics. The Western Alps are the most elevated and they are primarily influenced by air masses that flow from the Atlantic Ocean. This region presents several drilled sites (e.g. in the Monte Bianco and Monte

Rosa massifs). The glaciers of the Central Alps are less elevated compared with those in the Western Alps and they are threatened by rapid melting. In this region, drilled sites are limited in the area of the Ortles massif. Although the eastern part of the Alpine chain is influenced by cold air from Siberia, the presence of drilled sites is very low.

The Asian High Mountains correspond to the regions of Himalaya, Karakoram, Tibet, Pamir, Tien Shan and Altay Shan. The maximum elevation is the Mount Everest (8848 m) located at the border between China and Nepal. The main weather systems that influence the Asian High Mountains are the westerlies and the Indian monsoon. These systems produce regional climate patterns affecting glacier behaviour differently across the Asian High Mountains (Kääb and others, 2012; Yao and others, 2012; Mölg and others, 2013). The Indian monsoon supplies high amounts of precipitation from the Indian Ocean over the Himalaya (Gadgil, 2003). The westerlies system becomes more important in the Western Himalaya and the Karakoram. The northern and western air masses that flow from Siberia and Central Asia to the Tien Shan and Pamir Mountains dictate the continental climate of these regions.

3.1. Data harmonization and variable selection

3.1.1. Ice-Core Database

The Ice-Core Database (IDB) was created collecting ice-core data from the Tropical Ice cores Paleoclimatology database

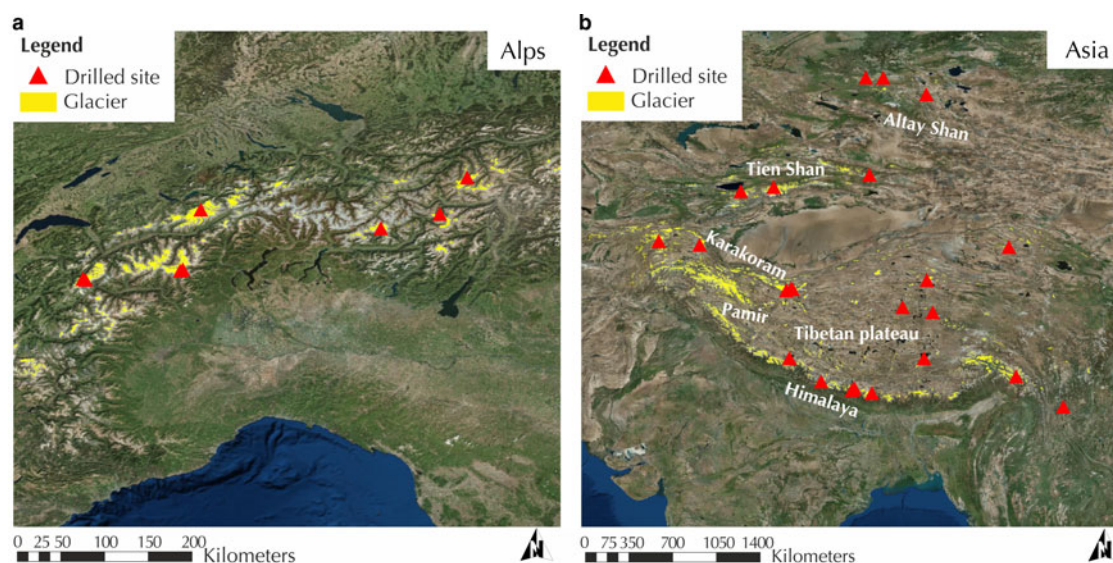


Fig. 1. Study area: the European Alps (a) and the Asian High Mountains (b). The yellow polygons show the extent of glaciers, with the position of the ice-core drilled sites (red triangles) retrieved from the Ice Core Database (IDB).

(National Oceanic and Atmospheric Administration, <http://www.ncdc.noaa.gov/paleo/icgate.html>), the US National Ice Core Laboratory (<http://www.icecores.org>), and through a detailed review of the scientific literature (Mattavelli and others, 2016). IDB was used for this study because it was the most complete archive of data from non-polar ice cores. We employed 24 drilled sites in the Alps and 42 in the Asian High Mountains (Table 2), where a total of 114 ice cores were collected.

3.1.2. Glacier outlines

The Randolph Glacier Inventory (RGI 4.0; Pfeffer and others, 2014) was used to define glacier outlines within the study area. This inventory is a globally complete collection of glacier outlines supplemental to the Global Land Ice Measurements from Space (Kargel and others, 2014). The European Alps contain 3812 glaciers, covering a total surface area of $\sim 2052 \text{ km}^2$, with a vertical altitudinal range from ~ 1500 to 4800 m . The Asian High Mountains include 85492 glaciers covering $\sim 120\,070 \text{ km}^2$, with an elevation range from 2500 to 8800 m .

3.1.3. Digital elevation model

The Advanced Spaceborne Thermal Emission and Reflection Radiometer (ASTER) Global Digital Elevation Model (ASTER G-DEM), characterized by 30 m spatial resolution (~ 1 arc-second) and $\sim 15\text{--}30 \text{ m}$ vertical accuracy (Tachikawa and others, 2011), was chosen in order to obtain global coverage with a homogeneous spatial resolution. This digital elevation model offers great geomorphologic detail in areas with a complex topography (Bolch and others, 2005; Hayakawa and others, 2008).

3.1.4. Climate data

Climate data were sourced from the WorldClim database. WorldClim is a set of global climatic data layers, with a spatial resolution of $\sim 1 \text{ km}^2$, generated through interpolation

of average monthly data from weather stations (1960–90 period; Hijmans and others, 2005). The most relevant variables for this study are monthly and annual precipitation, monthly mean, minimum and maximum temperature and some derived variables (e.g. mean diurnal range, mean temperature of warmest season, precipitation seasonality, precipitation of warmest season).

3.1.5. Selected morphometric and climatic variables

The most relevant morphometric and climatic variables to be used as input of the SICD model were identified based on a literature review combined with a preliminary analysis of the cumulative distribution functions (CDF) of the variables characterising the drilled sites present in the IDB. The values of each variable map were extracted from drilled sites (area of 5×5 pixels around the drilled point, $\sim 150 \text{ m} \times 150 \text{ m}$) and from RGI glacier polygons. Differences between the CDF of already drilled sites and the CDF of the whole glacier area were evaluated to characterize drilled sites. The following variables were selected:

- **Slope** ($^\circ$). Degree of surface inclination from the horizontal plane generated from DEM using a GIS (Geographic Information System) function (Hofierka and others, 2009). In areas with lower slope gradients, the preserved stratigraphy shows parallel layers that can easily refer to climate history. These sites are also suitable for technical drilling operations (e.g. location of drilling camp, drill requirements).
- **Local relief** (m). Vertical difference in elevation between the highest and lowest points of a land surface within a specified horizontal distance (computational window of 9×9 pixels; Wilson and Gallant, 2000). Higher values indicate the presence of steepest slopes that correspond to a major glacier flow velocity. These areas do not favour ice-core drillings because these elements can modify the original stratigraphy. In addition, steep slopes are also predisposing factors for avalanches, which disrupt the layers and constitute a risk for the technical operations.
- **Mean temperature of warmest season** ($^\circ\text{C}$). Average temperature of the three warmest months. The suitable areas for ice-core drilling are characterized by below freezing temperature throughout most of the year. As temperature is inversely correlated with elevation, drilling sites are generally chosen in more elevated areas. Conversely, positive temperatures (higher than 0°C) favour snow melting that can modify the ice-core stratigraphy. The mean temperature of warmest season was chosen from the WorldClim dataset in order to evaluate the mean higher temperature at the site.
- **Direct solar radiation** ($\text{W m}^{-2} \text{ d}^{-1}$). A raster map of solar direct radiation was calculated using the GIS software Geographic Resources Analysis Support System (GRASS) for a given day, latitude, surface and atmospheric condition (i.e. r.sun function; Hofierka and Šúri, 2002). This variable was computed considering topographic exposure and shadows and allows evaluation of temperature difference at local scale. The function was evaluated on 15 August. In this period, the mean temperatures are usually high in both study areas, and heat accumulation in the glacier body causes ice melting. Suitable areas for ice-core drilling are ideally those that are less exposed to high-intensity solar radiation.

Table 2. Ice-core drilling sites used in this study

European Alps	Number of drilled site
Ortles-Cevedale	1
Mount Blanc	7
Monte Rosa	11
Bernese-Oberland	1
Bernina-Morteratsch	1
Oetztal Alps	3
Total	24
Asian High Mountains	Number of drilled site
Altay and Sayan	4
Pamir (Safed Khirs)	3
Western Tien Shan	4
Eastern Tien Shan (Dzhungaria)	2
Western Kun Lun	7
Eastern Kun Lun (Altyn Tagh)	1
Qilian Shan	4
Inner Tibet	6
Central Himalaya	7
Eastern Himalaya	1
Hengduan Shan	3
Total	42

3.2. Weight of evidence and derivation of the SICD index

The SICD of mountain glaciers was defined here as the possibility of extracting an ice core with preserved stratigraphy suitable for reconstructing past climate conditions. SICD index was derived from a combination of the environmental variables described in Section 3.1.5 based on a Spatial Multi-criteria Analysis (Karnatak and others, 2007). Assuming that areas suitable for future drilling have similar conditions (i.e. combination of variables) to already drilled areas, the Weight of Evidence (WoE) method was proposed for analysing the drilling suitability of different sites. In order to apply the spatial analysis, each variable was divided into eight uniform intervals on the basis of the CDF (Table 3).

3.2.1. WoE method

A quantitative WoE scoring system was developed in this research to assign a weight to every interval of each variable used in the model and to spatially combine variables into a single value referred to as the SICD index. Similar approaches have been used mainly in geology to identify mineral potential (Bonham-Carter and others, 1989;

Agterberg and others, 1990) and for landslide susceptibility mapping (Thiery and others, 2007; Regmi and others, 2010). With this method, the spatial relationship between a variable and SICD is evaluated using a statistical approach based on the Bayesian probability theorem as follows:

$$P\{D|B\} = \frac{P\{B|D\} \times P\{D\}}{P\{B\}}$$

In this formula, the posterior probability $P\{D|B\}$ of locating a drilling site D within a specific variable interval B is equal to the product between the likelihood $P\{B|D\}$ of observing the variable interval B in a given drilling site D and the prior probability $P\{D\}$ of finding a drilling site, divided by the prior probability $P\{B\}$ of observing the variable interval (Regmi and others, 2010). Our model is based on the calculation of positive (W^+) and negative (W^-) weights for each variable interval as follows:

$$W^+ = \log_e \frac{P\{B|D\}}{P\{\bar{B}|D\}} \quad W^- = \log_e \frac{P\{\bar{B}|D\}}{P\{B|D\}}$$

where \bar{D} denotes the absence of an observed drilling site and \bar{B} indicates that the value of the variable is outside the considered interval. The difference between positive and negative

Table 3. Model parameters for the study areas of the European Alps and Asia. The table reports the positive and negative weights (W^+ and W^-) and the total weight (W^t) assigned to each interval of the selected variables (slope, local relief, mean temperature of warmest season, direct solar radiation) with the WoE method

Alps				Asia			
Variable interval	W^+	W^-	W^t	Variable interval	W^+	W^-	W^t
<i>Slope (°)</i>							
>35	-3.123	0.146	-3.269	>35	-1.659	0.245	-1.904
30-35	-1.058	0.067	-1.125	30-35	-1.797	0.088	-1.885
25-35	-0.839	0.081	-0.920	25-35	-1.229	0.081	-1.310
20-25	-0.328	0.049	-0.377	20-25	-0.647	0.059	-0.706
15-20	0.174	-0.037	0.211	15-20	0.402	-0.072	0.474
10-15	0.460	-0.112	0.572	10-15	0.807	-0.209	1.016
5-10	0.676	-0.141	0.817	5-10	0.797	-0.178	0.975
<5	0.998	-0.086	1.084	<5	0.686	-0.055	0.741
<i>Local relief (m)</i>							
>90	-1.431	0.435	-1.867	>90	-1.865	0.676	-2.541
80-90	-0.659	0.041	-0.700	80-90	-0.416	0.021	-0.437
70-80	-0.881	0.053	-0.934	70-80	-0.221	0.013	-0.234
60-70	0.121	-0.012	0.133	60-70	0.238	-0.019	0.257
50-60	0.628	-0.085	0.713	50-60	0.767	-0.092	0.859
40-50	0.874	-0.137	1.011	40-50	1.164	-0.195	1.359
30-40	1.325	-0.270	1.595	30-40	1.365	-0.250	1.615
<30	-0.205	0.016	-0.221	<30	0.200	-0.015	0.215
<i>Mean temperature of warmest season (°C)</i>							
>2	-	0.933	-	>4	-2.839	0.513	-3.352
1-2	-0.205	0.041	-0.245	3-4	-0.641	0.073	-0.714
0-1	-	0.119	-	2-3	0.081	-0.013	0.094
-1 to 0	-	0.054	-	1-2	-1.627	0.107	-1.734
-2 to -1	1.318	-0.082	1.399	0-1	0.724	-0.115	0.838
-3 to -2	0.929	-0.018	0.947	-1 to 0	1.716	-0.286	2.002
-4 to -3	4.730	-0.541	5.271	-2 to 1	1.654	-0.104	1.759
<-4	5.112	-0.351	5.463	<-2	1.894	-0.124	2.018
<i>Direct solar radiation ($W m^{-2} d^{-1}$)</i>							
>8240	1.927	-0.033	1.960	>8840	2.906	-0.049	2.956
7950-8240	0.615	-0.050	0.665	8450-8840	1.012	-0.199	1.210
7660-7950	1.018	-0.183	1.201	8060-8450	0.385	-0.105	0.491
7370-7660	0.796	-0.151	0.947	7670-8060	-0.344	0.061	-0.404
7080-7370	0.277	-0.040	0.317	7280-7670	-0.648	0.076	-0.724
6790-7080	-0.058	0.006	-0.064	6890-7280	-0.291	0.029	-0.320
6500-6790	-0.150	0.014	-0.164	6500-6890	-0.143	0.011	-0.154
<6500	-1.743	0.518	-2.262	<6500	-0.932	0.164	-1.097

weights is the total weight $W^t = W^+ - W^-$, which provides a measure of the spatial association between variable intervals and observed drilling sites.

The WoE method was applied treating separately the two areas of study. Drilled sites (i.e. area of 5×5 pixels around the drilled point) were overlapped with variable maps, and only the area of glacier extension was considered as total area of study.

3.2.2 SICD index derivation

The SICD index was calculated using a linear combination of weights defined for the selected variables:

$$SICD_{WoE} = S_{W^t} + R_{W^t} + T_{W^t} + D_{W^t},$$

where S, R, T, D are the four variables (Slope, local Relief, Temperature, Direct radiation) and W^t is the total weight corresponding to the variable interval calculated using the WoE method. All variable maps were combined in a GIS environment (i.e. GRASS). The SICD index maps were created for the European Alps and for the Asian High Mountain glaciers. Higher values of SICD indicate a better site for ice-core drilling. Normalization (between 0 and 1) was performed for the maps of SICD to evaluate the model. Finally, the first indications of potential glaciers suitable for ice-core drilling were established by ranking the sum of pixels with values of SICD >0.7 of a glacier.

3.3 Model evaluation

The root-mean-square error (RMSE) was computed to evaluate the generated maps. It was calculated using the values of SICD estimated at the drilled sites and considering 1 the expected value of SICD at these points. Furthermore, the ability of the proposed method to indicate suitable areas for ice-core drilling was verified using the success rate curve to evaluate the goodness of fit of the model (Pradhan and others, 2010; Sterlacchini and others, 2011). The success rate curve indicates how well the model fits the occurrences by calculating the percentage of drilled sites that occur in the areas classified with higher values of SICD. If the curve and the diagonal coincide, the model should be deemed equivalent to a totally random model. Likewise, greater slope in the first part of the curve indicates higher model quality. The curve was created by cross-checking the distribution of the total set of drilled sites with the SICD maps: after sorting SICD values of each pixel in descending order, the cumulative percentage of drilled sites was plotted against the cumulative percentage of the total study area. The area under the curve (AUC) represents the quality of the model to reliably fit the occurrence: the larger the area, the greater is the goodness of fit of the model. The AUC allows the comparison of different success rate curves. A total area equal to 100 denotes perfect accuracy, whereas values below 50 represent a random fit.

4. RESULTS AND DISCUSSION

4.1. Spatial variability of the selected variables

The spatial variability of the selected variables is shown in Figure 2, focusing on the Monte Rosa massif (European Alps). Low slope values ($0-20^\circ$) are present in glacier tongues but also in more elevated areas in the accumulation

basins suitable for ice-core drilling (Fig. 2a). High local relief values (higher than 70 m) are found along the mountain ridges and in the vicinity of northern sides (Fig. 2b). Those steep slopes are generally associated with stratigraphic deformation of seasonal depositions. The mean temperature of the warmest season (Fig. 2c) shows an inverse relation with elevation, with negative temperatures in the more elevated summit areas. The local variability typical of complex mountain ranges is better resolved in the direct solar radiation map (Fig. 2d, 30 m spatial resolution) with respect to the temperature map (Fig. 2c, 1 km spatial resolution). The highest values of solar radiation are observed on elevated flat areas and southern slopes because they are not shielded by the effect of topography (i.e. prevailing exposure and shadows).

Figure 3 shows the CDF of each variable at the drilled sites. The curve enables us to determine which values characterize the drilled sites. Based on the CDF, each variable was divided into the same uniform intervals used in the WoE model (Table 3). CDF plots of slope and local relief show similar behaviour between the Alps and the Asian High Mountains, whereas some differences are present for mean temperature and direct solar radiation. Regarding the slope, we observe that 80% of the drilling sites are characterized by values lower than 20° (Fig. 3a). Local relief CDF shows that the drilled sites are mainly characterized by low values of local relief (Fig. 3b). Mean temperature of warmest season (Fig. 3c) in the drilled Alpine sites ranges from -4°C to 2°C , with 85% of the sites having a mean temperature lower than 0°C , while for the Asian glaciers the temperature CDF shifts to higher values ranging from -2°C to 4°C . Similar differences can be observed for direct radiation (Fig. 4d). These can be ascribed to geomorphological differences between the Alps and the Asian High Mountains. The latter, in fact, cover a broader altitudinal and latitudinal range, resulting in higher temperature and direct radiation than in the European Alps. These differences were considered in order to adjust the intervals used for these variables in the two study areas.

4.2. Weight definition

The results of the WoE are shown in Table 3. Variable intervals with negative weights are negatively associated with SICD, while positive values indicate that the identification of variables within the specified intervals favours ice-core drilling. Weights close to zero reveal a slight relation between the interval and SICD. Weight values between the Alps and the Asian region show good agreement. Low slope values ($0-15^\circ$) have positive weights, indicating that these intervals are suitable for ice-core drilling, whereas values above 25° are negatively related with SICD. Local relief shows that values from 30 to 50 m are positively associated with SICD while high values (>70 m) are less favourable (negative weights) to ice-core drilling. The WoE model shows that areas more exposed to solar radiation evidence a positive relation with SICD. Finally, temperature is the most important variable with the highest weights for low-temperature values.

4.3. SICD maps and model evaluation

Figure 4 shows a focus of the SICD map on the Monte Rosa Massif (Central Alps) and on Dasuopu and Yala glaciers (Central Himalaya). Green colour indicates areas not suitable

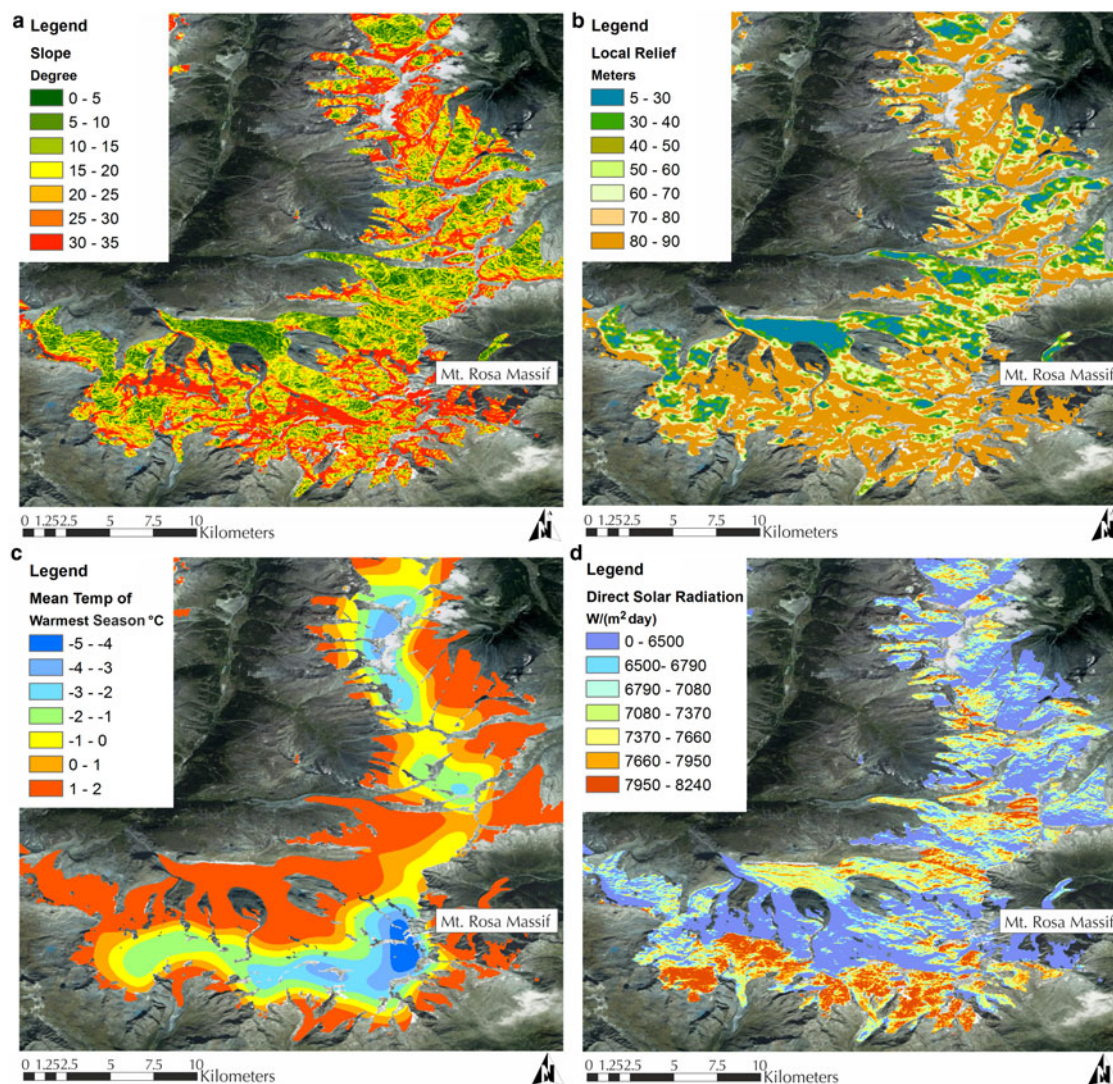


Fig. 2. Environmental variables included in the model: (a) slope; (b) local relief; (c) mean temperature of warmest season; (d) direct solar radiation. Example for the Monte Rosa massif, European Alps.

for ice-core drilling; yellow and orange colours evidence sites with moderate SICD; red indicates potential drilling sites corresponding to high values of SICD (i.e. 0.7–1). Blue triangles in the maps show the locations of already drilled sites.

Areas suitable for ice-core drilling, identified with red colour on the map, are mostly located in elevated flat areas, whereas southern-exposed glaciers and steep northern slopes are usually characterized by lower SICD values.

The evaluation of model performances was separately conducted for the two study areas. The mean values of SICD in the already drilled sites are equal to 0.75 and 0.70 in the Alps and in Asia, respectively. The RMSE values are 0.29 for the Alps and 0.35 for Asia. The AUC, representing the quality of the model to reliably fit the occurrence, assumes values of 95.86 in the Alps and 89.77 in the Asian region. More in detail, the success rate curve (Fig. 5) shows that 13% of the study area classified as more suitable for ice-core drilling (i.e. higher SICD values) contains 90% of the already drilled sites (red line) in the Alps, while, for the Asian High Mountains, 21% of the most suitable area contains 90% of the drilled sites (blue line).

All these results suggest that the model performs well in both study areas, with slightly better performances in the Alps compared with the Asian mountains. In the European Alps, hotspots of high SICD values correspond to the areas where the already drilled sites are located. This result confirms that all the potential drilling sites have been already exploited in the Alps and allows to verify the reliability of the proposed method in providing SICD maps. In contrast, in the Asian region, hotspots of high SICD values are located both in correspondence to already drilled sites and in still unexplored areas, suggesting that several new potential drilling sites can be identified in the High Asian Mountains using the model proposed in this study.

As examples of potential drilling areas in the Asian High Mountains, Figure 6 shows true colour Landsat 8 images and the SICD map zoomed, respectively, in Central Himalaya (Fig. 6a), Karakoram (Fig. 6b) and Altay mountains in Tien Shan (Fig. 6c). Red colours indicate SICD values ranging from 0.7 to 1 and represent most suitable drilling areas.

The proposed methodology combines morphometric and climatic variables that are globally and freely distributed from online repositories. Some limitations of the model could be

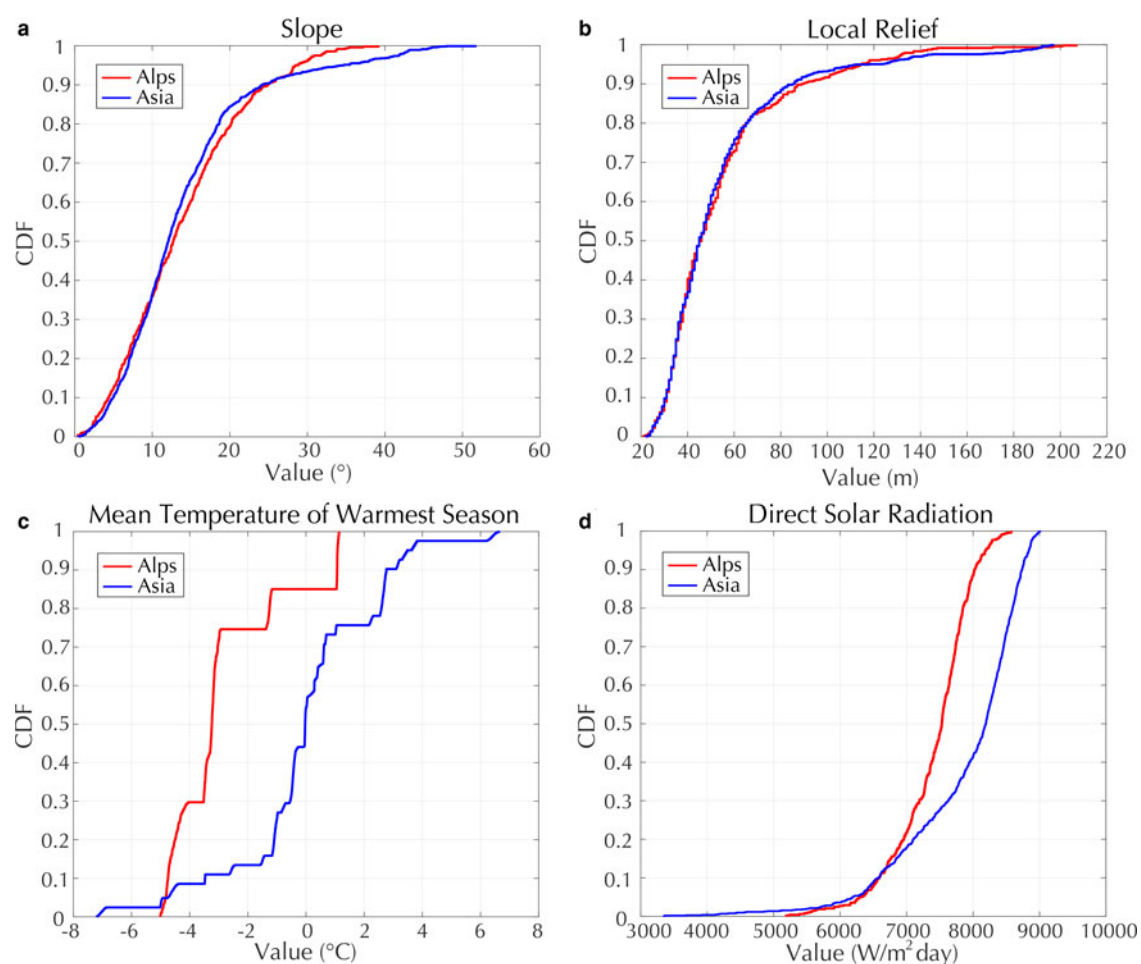


Fig. 3. Cumulative distribution functions (CDF) of selected variables for Alps (red line) and Asia (blue line). The curves show the distribution of values of each variable at all the available drilling sites. (a) slope; (b) local relief; (c) mean temperature of warmest season; (d) direct solar radiation.

caused by the accuracy of the ASTER G-DEM and RGI glacier outlines. ASTER G-DEM shows a vertical accuracy of ~15–30 m that can introduce errors in the morphometric variables. This product was chosen in order to have a global DEM with high spatial resolution. DEM artefacts (e.g. spikes, holes, etc.) can in principle affect the SICD analysis. We overcome this issue by considering an area of 9×9 pixels when calculating morphometric variables. Furthermore, when evaluating SICD maps, we considered as potential drilling sites only parts of the glacier characterized by a cluster of high SICD values.

Model inaccuracies can arise also from the use of the RGI dataset to define glacier outlines. Artefacts such as internal rocks or snow-covered bedrock are included in the RGI dataset. However, despite this limitation, the RGI was chosen because it is the most complete database of glacier outlines. Another limitation of our model is the possibility of identifying high SICD values in large ablation zones (e.g. see Fig. 6a for the Central Himalaya). To overcome these issues, the selection of potential drilling sites was supported by the inspection of optical satellite images.

Other variables, such as glacier thickness, snow accumulation, wind erosion and warming trend, can also have an effect on the SICD definition. They are not included in the model because they are not globally distributed. These variables should be further investigated at regional or local scale to support the accurate location of a drilling site within a

suitable area. For example, glacier thickness is a very important variable because it is directly related to the stratigraphic resolution and it is traditionally explored using ground-penetrating radar soundings or with physical methods based on surface slope and driving stress (Hoelzle and others, 2007; Cuffey and Paterson, 2010).

4.4. Discussion of potential drilling sites

Glaciers with most potential for ice-core drilling were identified by summing SICD values higher than 0.7 for glacier polygons in the following geographic regions (Table 4): Central Himalaya, Hengduan Shan, East Himalaya, Hindu Kush, West Himalaya, Central Himalaya, Karakoram, Pamir, South and Est Tibet, Inner Tibet, East Kun Lun, East Tien Shan, West Kun Lun, West Tien Shan, Alps (Mt. Rosa), Alps (Bernina), Alps (Aletsch), Alps (Mt. Bianco) and Alps (Grossfiescherhorn). Table 4 shows also that our model performs well in the Alps, in fact the locations of potential drilling areas identified by the model reflect the position of already drilled sites.

The SICD map highlights the presence of unexplored glaciers suitable for ice-core drilling in the Asian High Mountains that should be exploited in the next years for collecting fundamental climatic and environmental data. Figure 7 shows the location of the most suitable glaciers (blue dots) and the already drilled sites (red triangles) for

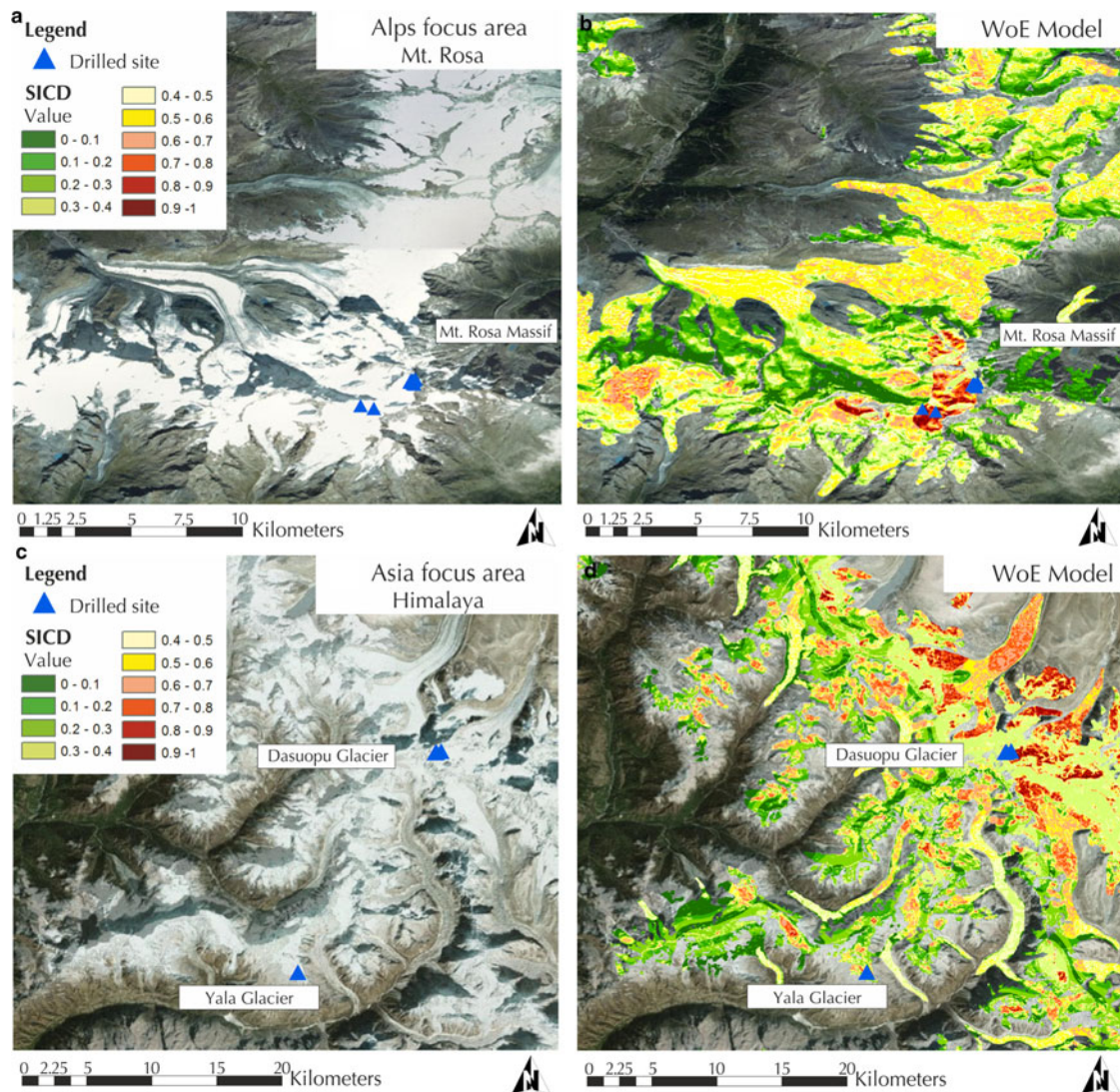


Fig. 4. Focus of true colour Landsat 8 images (left column) and related suitability for ice-core drilling maps (right column) in Alpine and Asian regions. (a) Focus on Monte Rosa Massif (Col du Lys and Colle Gnifetti drilling site) in the European Alps; (b) WoE SICD map of Monte Rosa Massif; (c) Focus on Dasuopu and Yala glaciers in Himalaya; (d) WoE SICD map of Dasuopu and Yala glaciers. Green is associated with areas unsuitable for ice-core drilling, yellow and orange colours show moderate SICD, and red indicates potential drilling sites, corresponding to high values of suitability for ice-core drilling (0.7–1). Blue triangles show the locations of already drilled sites.

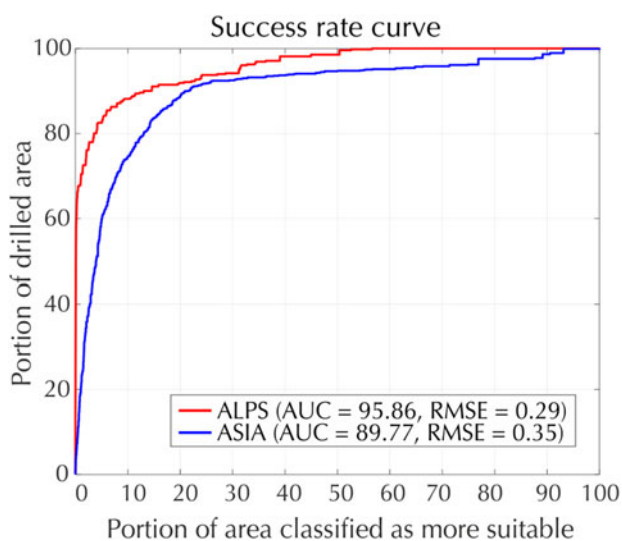


Fig. 5. Success-rate curves, area under the curve (AUC) values and root-mean-square error computed for the Alps (red line) and the Asian High Mountains (blue line).

each geographic region of the Asian High Mountains as defined in the RGI dataset.

Hereafter, we illustrate the usefulness of this approach by highlighting some specific areas in Asia evidenced by the SICD map (Fig. 7), which are expected to provide valuable scientific information. First of all, the realization of new drilling sites in the Himalayan glaciers could provide further insights on the activity of the Indian monsoon system (Benn and Owen, 1998). This system showed a variation over the last decades corresponding to a decreasing trend in precipitation and snowfall and an increasing trend of temperatures over the Himalayan mountain ranges (Bhutiyan and others, 2007; Shekhar and others, 2010; Singh and Mal, 2014). These variations are recorded in the ice-core stratigraphy (Zhisheng and others, 2001; Kaspari and others, 2007; Sinha and others, 2015). Some drillings have been performed in the Himalaya, but many sites should be exploited in the coming years. The glaciers are rapidly shrinking with an expected higher trend in the next years (Bolch and others, 2012; Kang and others, 2015). Consequently, potential sites have the highest drilling priority if compared with the other Asian regions.

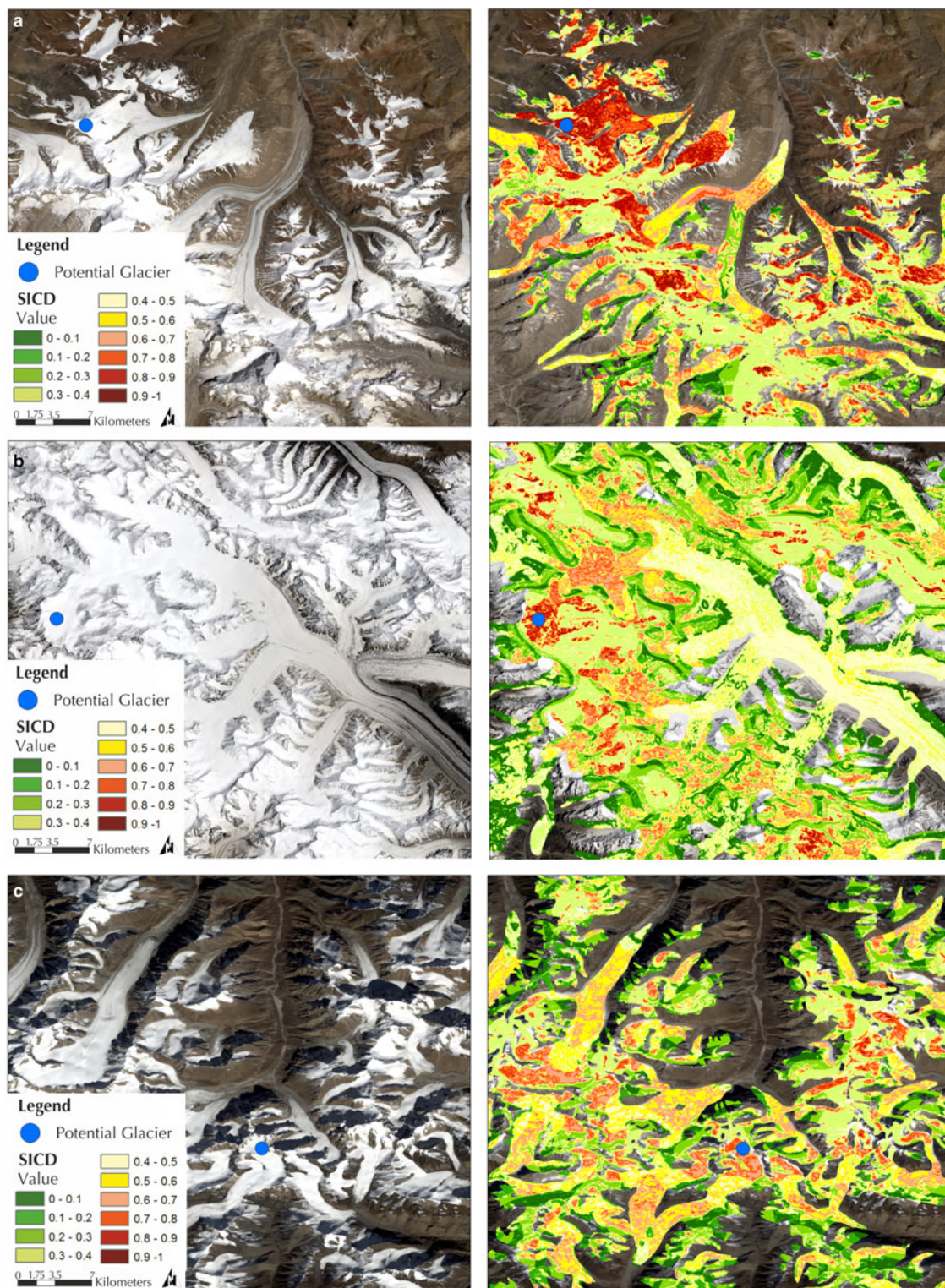


Fig. 6. True colour Landsat 8 images (left column) and maps of suitability for ice-core drilling (SICD) (right column) for the Asian High Mountains glaciers: (a) Central Himalaya, (b) Karakoram region and (c) Altay mountains in Tien Shan. The areas with drilling potential (blue dots) correspond to high values of SICD (red colours).

In easternmost parts of the Himalaya, other glaciers with drilling potential receive the contribution of the Southeast Asian air masses influenced by densely inhabited areas (i.e. China, India). New drilling sites in this region could thus provide valuable information on the effects of anthropogenic activities (i.e. emission of pollutants, aerosol, black carbon, soluble ions) and their impacts on the environment (e.g. glacier retreat and corresponding variation of seasonal fresh water supplies; Hong and others, 2009; Xu and others,

2009; Zhao and others, 2011). These new climatic and environmental archives could be exploited to compare the anthropogenic emissions due to Asian emerging economies with the emissions coming from other industrialized regions (e.g. Europe or America; Duan and others, 2007; Kaspari and others, 2009a, b).

The western region of the Karakoram is poorly explored and, to date, only shallow ice cores (Wake, 1989) and snow pits (Mayer and others, 2014) have been studied. In

Table 4. Asian High Mountains and European Alps glaciers suitable for ice-core drilling as identified by summing SICD values higher than 0.7 within the RGI glacier polygons. Glaciers are ranked according to the sum of the SICD values

	Geographic region	Latitude (deg)	Longitude (deg)	Elevation (m)	RGI-ID
Asian High Mountains (RGI regions)	Central Himalaya	29.1390008	83.68951757	5893	RGI40-15.04438
	Hengduan Shan	29.38275094	96.53840206	5576	RGI40-15.11438
	East Himalaya	28.08806426	86.76204418	6301	RGI40-15.13894
	Hindu Kush	36.36168995	71.74722481	5541	RGI40-14.00009
	West Himalaya	34.00099313	76.05439232	6036	RGI40-14.19703
	Central Himalaya	31.06786452	79.48840859	6296	RGI40-14.21821
	Karakoram	35.54050774	76.7618348	6089	RGI40-14.22774
	Pamir	38.54728651	72.35499671	5725	RGI40-13.02225
	South and East Tibet	31.81391302	94.69375025	6130	RGI40-13.12908
	Inner Tibet	34.36457491	85.86503518	6082	RGI40-13.16215
	Inner Tibet	33.91626201	89.16452314	5983	RGI40-13.16427
	East Kun Lun	36.08073392	90.971344	5635	RGI40-13.16696
	East Tien Shan	43.5118212	85.24638223	4507	RGI40-13.27269
	West Kun Lun	35.3342849	80.81203255	6396	RGI40-13.38172
West Tien Shan	42.08041205	80.2515314	5667	RGI40-13.42410	
European Alps	Alps (Mt. Rosa)	45.9206556	7.822309248	3984	RGI40-11.02973
	Alps (Bernina)	46.37585896	9.949741763	3647	RGI40-11.02173
	Alps (Aletsch)	46.54908372	7.991921247	3504	RGI40-11.01450
	Alps (Mt. Bianco)	45.8389896	6.868924542	4459	RGI40-11.03076
	Alps (Mt. Bianco)	45.84446435	6.846433797	4263	RGI40-11.03030
	Alps (Grossfiescherhorn)	46.54866971	8.071081852	3898	RGI40-11.01478

contrast to the Himalaya, the Karakoram range shows great potential in studying variations of winter precipitation in relation with the North Atlantic Oscillation (NAO) and the El Niño–Southern Oscillation (ENSO; Filippi and others, 2014; Cannon and others, 2016). NAO and ENSO were already detected from isotopic composition in several Tibetan Plateau ice cores (Joswiak and others, 2013; Yang and others, 2014; Du and others, 2016). In this context, ice-core records are fundamental for modelling the impacts

of NAO and ENSO on regional and global circulation patterns (Kumar and others, 2015; Dixit and Tandon, 2016). This is important because NAO and ENSO have strong effects on mid-latitude circulation patterns that impact large regions of the planet (Brönnimann and others, 2006; Müller and Roeckner, 2006; Donat and others, 2014; Whan and Zwiers, 2017). In addition, the Karakoram region shows a decreasing trend in maximum and minimum temperatures, together with an increase in winter precipitations. Glaciers

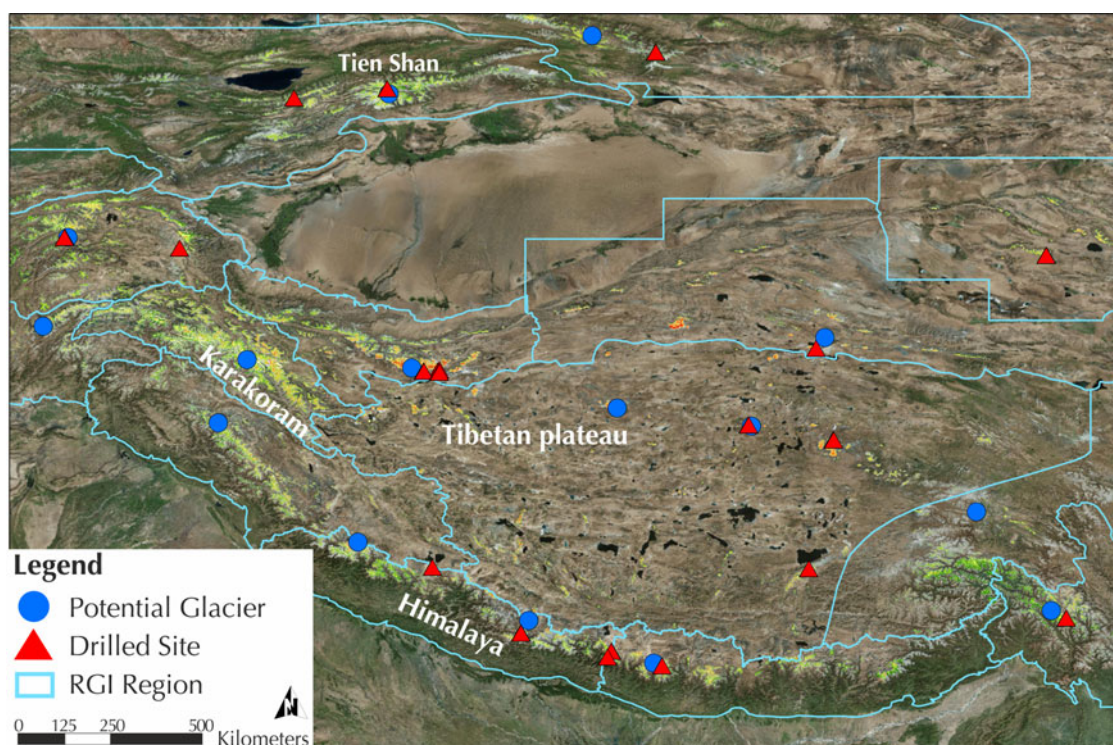


Fig. 7. Glaciers with the highest potential for ice-core drilling (blue dots), and position of the already drilled sites (red triangles) for each geographic region of the Asian High Mountains as defined in the RGI dataset.

exhibit evidences of expansion (i.e. the 'Karakoram anomaly') in contrast to a worldwide decline (Fowler and others, 2006; Bolch and others, 2012; Gardelle and others, 2012). For this reason, they are less threatened by warming and they can provide more seasonal resolved records.

The climate of the Tibetan Plateau is dry and isolated from the other Asian regions (Kang and others, 2010). This wide region is recognized to be a heat source during the summer season that drives both regional and general circulation (Ye and Wu, 1998; Duan and Wu, 2005). New ice cores can be useful for studying the regional recent warming (An and others, 2016), or the mineral dust transport and deposition (Kang and others, 2003). For example, atmospheric depositions of impurities (such as black carbon and mineral dust) can decrease the albedo of snow and ice promoting the melt (Qu and others, 2014; Di Mauro and others, 2015). This process can be studied using ice cores to evaluate the possible impact on glacier albedo reduction (Xu and others, 2009; Kaspari and others, 2009a, b).

Finally, air masses that flow from Siberia and Central Asia to the Tien Shan and Pamir Mountains characterize the continental climate of these northern regions (Aizen and others, 2006; Papina and others, 2013). The glaciers with drilling potential in the Altay mountains and Tien Shan could be investigated in order to understand regional and large-scale transports of dust or pollutants related to regional economic activities (Kreutz and others, 2001; Lee and others, 2003; Grigholm and others, 2016). The Pamirs Plateau is dominated by a relatively simple atmospheric circulation system (i.e. the westerlies); therefore, it can show remarkable differences compared with southern Tibetan Plateau or Himalaya (i.e. combined effects of westerlies and monsoon). This region can be an ideal location for obtaining robust proxy reconstructions of differences in past temperatures and circulation dynamics between the Asian regions (Aizen and others, 2006; Yu and others, 2016).

5. CONCLUSIONS

Ice cores recovered from mid-latitude mountain glaciers are excellent archives for understanding recent climatic and environmental variability related to anthropogenic factors. From this point of view, they offer advantages if compared with polar ice cores. Documented rapid glacier retreat makes urgent the identification of new potential drilling sites. To date, the criteria for identifying suitable areas and choosing drilling sites have not been addressed quantitatively in the scientific literature.

In this work, we proposed a first step towards developing a methodology to assess the suitability of mountain glaciers for ice-core drilling, in order to collect ice cores with preserved stratigraphy. We optimized the WoE method for mapping the SICD of glaciers in unexplored areas. First, we created and evaluated the model in the European Alps, then we applied the methodology in the Asian High Mountains. The first maps of SICD were thus proposed. Useful indications for the selection of the next drilling sites were provided for the Asian High Mountains, underlining their scientific potential in studying regional climate variability, anthropogenic impacts and global climate circulations. Our results could be especially relevant in this unexplored area where little information is available and many potential drilling sites are still to be exploited. Our results also pave the way to the development of automatic classification methods to

map the SICD in other poorly explored mountain ranges. In the future, the incorporation of other variables (e.g. glacier thickness, snow accumulation, wind erosion and warming trend) in the model will allow improving SICD estimations.

ACKNOWLEDGEMENTS

The present study was performed in the framework of the Project of Interest NextData: a national system devoted to assessing the effects of climate and environmental change in mountain areas. We thank G. Orombelli, B. Delmonte, G. Baccolo, M. Filipazzi, M. Mattavelli, M. Moretti (DISAT-UNIMIB, Italy) and all the Cryolist members that kindly compiled the questionnaire we created to initiate this research. We thank the anonymous reviewers and the Scientific Editor for their work and their useful comments and suggestions that helped us in improving the quality of the manuscript. The complete map of SICD map is accessible upon the request to the corresponding author.

AUTHOR CONTRIBUTIONS

RG and BDM performed the data analysis, developed the methodology and wrote the paper with the contribution of all the authors. MR and RC contributed to the interpretation of results. DS and MDA developed the Ice-Core Database and GIS implementations. VM was the project coordinator.

REFERENCES

- Agterberg FP, Bonham-Carter GF and Wright DF (1990) Statistical pattern integration for mineral exploration, in Gàal, G., and Merriam, D. F., eds., *Computer Applications in Resource Estimation*. Pergamon, Oxford, p. 1–21
- Aizen VB and 5 others (2006) Climatic and atmospheric circulation pattern variability from ice-core isotope/geochemistry records (Altai, Tien Shan and Tibet). *Ann. Glaciol.*, **43**(1), 49–60 (doi: 10.3189/172756406781812078)
- Alley RB (2000) Ice-core evidence of abrupt climate changes. *Proc. Natl. Acad. Sci.*, **97**(4), 1331–1334 (doi: 10.1073/pnas.97.4.1331)
- An W and 6 others (2016) Significant recent warming over the northern Tibetan Plateau from ice core δ 18 O records. *Clim. Past*, **12**, 201–211 (doi: 10.5194/cp-12-201-2016)
- Andersen KK and 48 others (2004) High-resolution record of Northern Hemisphere climate extending into the last interglacial period. *Nature*, **431**(7005), 147–151 (doi: 10.1038/nature02805)
- Beniston M (2005) Mountain climates and climatic change: an overview of processes focusing on the European Alps. *Pure Appl. Geophys.*, **162**(8–9), 1587–1606 (doi: 10.1007/s00024-005-2684-9)
- Benn DI and Owen LA (1998) The role of the Indian summer monsoon and the mid-latitude westerlies in Himalayan glaciation: review and speculative discussion. *J. Geol. Soc. London.*, **155**(2), 353–363 (doi: 10.1144/gsjgs.155.2.0353)
- Bhutiyan MR, Kale VS and Pawar NJ (2007) Long-term trends in maximum, minimum and mean annual air temperatures across the Northwestern Himalaya during the twentieth century. *Clim. Change*, **85**(1–2), 159–177 (doi: 10.1007/s10584-006-9196-1)
- Birnbaum G and 16 others (2010) Strong-wind events and their influence on the formation of snow dunes: observations from Kohlen station, Dronning Maud land, Antarctica. *J. Glaciol.*, **56**(199), 891–902 (doi: 10.3189/002214310794457272)
- Bolch T, Kamp U and Olsenholler J (2005) Using ASTER and SRTM DEMs for studying geomorphology and glaciation in high mountain areas. In Oluic (ed.), *New Strateg. Eur. Remote Sens.*, Millpress, Rotterdam 119–128 (doi: ISBN 90 5966 003 X)

- Bolch T and 11 others (2012) The state and fate of Himalayan glaciers. *Science*, **336**(6079), 310–314 (doi: 10.1126/science.1215828)
- Bonham-Carter GF, Agterberg FP and Wright DF (1989) Weights of evidence modelling: a new approach to mapping mineral potential. In Agterberg FP and Bonham-Carter GF, eds. *Statistical applications in the earth sciences*. Canadian Government Publishing Centre, Ottawa, 171–183
- Bronnimann S, Xoplaki E, Casty C, Pauling A and Luterbacher J (2006) ENSO influence on Europe during the last centuries. *Clim. Dyn.*, **28**(2–3), 181–197 (doi: 10.1007/s00382-006-0175-z)
- Buffen AM, Hastings MG, Thompson LG and Mosley-Thompson E (2014) Investigating the preservation of nitrate isotopic composition in a tropical ice core from the Quelccaya Ice Cap, Peru. *J. Geophys. Res. Atmos.*, **119**(5), 2674–2697 (doi: 10.1002/2013JD020715)
- Campbell S and 7 others (2012) Melt regimes, stratigraphy, flow dynamics and glaciochemistry of three glaciers in the Alaska range. *J. Glaciol.*, **58**(207), 99–109 (doi: 10.3189/2012JoG10J238)
- Cannon F and 6 others (2016) The influence of tropical forcing on extreme winter precipitation in the western Himalaya. *Clim. Dyn.*, **48**(3–4), 1213–1232 (doi: 10.1007/s00382-016-3137-0)
- Copland L and Sharp M (2001) Mapping thermal and hydrological conditions beneath a polythermal glacier with radio-echo sounding. *J. Glaciol.*, **47**(157), 232–242 (doi: 10.3189/172756501781832377)
- Cuffey K and Paterson WSB (2010) *The physics of glaciers*, 3rd edn. Butterworth-Heinemann/Elsevier Academic Press
- Davis ME and Thompson LG (2005) Forcing of the Asian monsoon on the Tibetan Plateau: evidence from high-resolution ice core and tropical coral records. *J. Geophys. Res. D Atmos.*, **110**(4), 1–13 (doi: 10.1029/2004JD004933)
- Delmas RJ (1992) Environmental information from ice cores. *Rev. Geophys.*, **30**(1), 1–21 (doi: 10.1029/91RG02725)
- Di Mauro B and 6 others (2015) Mineral dust impact on snow radiative properties in the European Alps combining ground, UAV, and satellite observations. *J. Geophys. Res. Atmos.*, **120**(12), 6080–6097 (doi: 10.1002/2015JD023287)
- Dixit Y and Tandon SK (2016) Hydroclimatic variability on the Indian subcontinent in the past millennium: review and assessment. *Earth-Sci. Rev.*, **161**, 1–15 (doi: 10.1016/j.earscirev.2016.08.001)
- Donat MG and 26 others (2014) Changes in extreme temperature and precipitation in the Arab region: long-term trends and variability related to ENSO and NAO. *Int. J. Climatol.*, **34**(3), 581–592 (doi: 10.1002/joc.3707)
- Döscher A, Göggele HW, Schotterer U and Schwikowski M (1995) A 130 years deposition record of sulfate, nitrate and chloride from a high-alpine glacier. *Water, Air, Soil Pollut.*, **85**(2), 603–609 (doi: 10.1007/BF00476895)
- Du W, Kang S, Qin X, Cui X and Sun W (2016) Atmospheric insight to climatic signals of δO in a Laohugou ice core in the north-eastern Tibetan Plateau during 1960–2006. *Sci. Cold Arid Reg.*, **8**(5), 367–377 (doi: 10.3724/SP.J.1226.2016.00367)
- Duan AM and Wu GX (2005) Role of the Tibetan Plateau thermal forcing in the summer climate patterns over subtropical Asia. *Clim. Dyn.*, **24**(7–8), 793–807 (doi: 10.1007/s00382-004-0488-8)
- Duan K, Thompson LG, Yao T, Davis ME and Mosley-Thompson E (2007) A 1000 year history of atmospheric sulfate concentrations in southern Asia as recorded by a Himalayan ice core. *Geophys. Res. Lett.*, **34**(1), L01810 (doi: 10.1029/2006GL027456)
- Epica CM (2004) Eight glacial cycles from an Antarctic ice core. *Nature* **429**(6992), 623–628 (doi: 10.1038/nature02599)
- Epica CM (2006) One-to-one coupling of glacial climate variability in Greenland and Antarctica. *Nature*, **444**(7116), 195–198 (doi: 10.1038/nature05301)
- Faria SH and 6 others (2009) *Multiscale structures in the Antarctic ice sheet part I: inland ice*. Takeo Hondoh Sapporo: Hokkaido University Press. (Low Temperature Science SI ed. Physics of ice core records II. (doi: 10013/epic.35759)
- Faria SH, Freitag J and Kipfstuhl S (2010) Polar ice structure and the integrity of ice-core paleoclimate records. *Quat. Sci. Rev.*, **29**(1), 338–351 (doi: 10.1016/j.quascirev.2009.10.016)
- Faria SH, Weikusat I and Azuma N (2014) The microstructure of polar ice. Part I: highlights from ice core research. *J. Struct. Geol.*, **61**, 2–20 (doi: 10.1016/j.jsg.2013.09.010)
- Filippi L and 7 others (2014) Multidecadal variations in the relationship between the NAO and winter precipitation in the Hindu Kush–Karakoram. *J. Clim.*, **27**(20), 7890–7902 (doi: 10.1175/JCLI-D-14-00286.1)
- Fowler HJ, Archer DR, Fowler HJ and Archer DR (2006) Conflicting signals of climatic change in the upper Indus basin. *J. Clim.*, **19**(17), 4276–4293 (doi: 10.1175/JCLI3860.1)
- Gabrielli P and 11 others (2010) Atmospheric warming threatens the untapped glacial archive of Ortles mountain, South Tyrol. *J. Glaciol.*, **56**(199), 843–853 (doi: 10.3189/002214310794457263)
- Gadgil S (2003) The Indian monsoon and its variability. *Annu. Rev. Earth Planet. Sci.*, **31**(1), 429–467 (doi: 10.1146/annurev.earth.31.100901.141251)
- Gardelle J, Berthier E and Arnaud Y (2012) Slight mass gain of Karakoram glaciers in the early twenty-first century. *Nat. Geosci.*, **5**(5), 322–325 (doi: 10.1038/ngeo1450)
- Grigholm B and 9 others (2016) Mid-twentieth century increases in anthropogenic Pb, Cd and Cu in Central Asia set in hemispheric perspective using Tien Shan ice core. *Atmos. Environ.*, **131**, 17–28 (doi: 10.1016/j.atmosenv.2016.01.030)
- Hayakawa YS, Oguchi T and Lin Z (2008) Comparison of new and existing global digital elevation models: ASTER G-DEM and SRTM-3. *Geophys. Res. Lett.*, **35**(17), L17404 (doi: 10.1029/2008GL035036)
- Hijmans RJ, Cameron SE, Parra JL, Jones PG and Jarvis A (2005) Very high resolution interpolated climate surfaces for global land areas. *Int. J. Climatol.*, **25**(15), 1965–1978 (doi: 10.1002/joc.1276)
- Hoelzle M and 5 others (2007) The application of glacier inventory data for estimating past climate change effects on mountain glaciers: a comparison between the European Alps and the Southern Alps of New Zealand. *Glob. Planet. Change*, **56**, 69–82 (doi: 10.1016/j.gloplacha.2006.07.001)
- Hofierka J and Šúri M (2002) *The solar radiation model for open source GIS: implementation and applications*. Open source GIS – GRASS users conference in Trento, Italy, September 2002
- Hofierka J, Mitášová H and Neteler M (2009) Chapter 17 geomorphometry in GRASS GIS. In Hengl T and Reuter HI, eds. *Developments in soil science*. Elsevier, Volume **33**, 387–410 (doi: 10.1016/S0166-2481(08)00017-2)
- Hong S and 8 others (2009) An 800-year record of atmospheric As, Mo, Sn, and Sb in Central Asia in high-altitude ice cores from Mt. Qomolangma (Everest), Himalayas. *Environ. Sci. Technol.*, **43**(21), 8060–8065 (doi: 10.1021/es901685u)
- Jenk TM and 7 others (2006) Radiocarbon analysis in an Alpine ice core: record of anthropogenic and biogenic contributions to carbonaceous aerosols in the past (1650–1940). *Atmos. Chem. Phys. Discuss.*, **6**(4), 5905–5931 (doi: 10.5194/acpd-6-5905-2006)
- Joswiak DR, Yao T, Wu G, Tian L and Xu B (2013) Ice-core evidence of westerly and monsoon moisture contributions in the central Tibetan Plateau. *J. Glaciol.*, **59**(213), 56–66 (doi: 10.3189/2013JoG12J035)
- Jouzel J and Masson-Delmotte V (2010) Paleoclimates: what do we learn from deep ice cores? *Wiley Interdiscip. Rev. Clim. Chang.*, **1**(5), 654–669 (doi: 10.1002/wcc.72)
- Kääb A, Berthier E, Nuth C, Gardelle J and Arnaud Y (2012) Contrasting patterns of early twenty-first-century glacier mass change in the Himalayas. *Nature*, **488**(7412), 495–498 (doi: 10.1038/nature11324)
- Kang S and 5 others (2003) Dust records from three ice cores: relationships to spring atmospheric circulation over the Northern

- Hemisphere. *Atmos. Environ.*, **37**(34), 4823–4835 (doi: 10.1016/j.atmosenv.2003.08.010)
- Kang S and 5 others (2010) Review of climate and cryospheric change in the Tibetan Plateau. *Environ. Res. Lett.*, **5**(1), 15101 (doi: 10.1088/1748-9326/5/1/015101)
- Kang S and 10 others (2015) Dramatic loss of glacier accumulation area on the Tibetan Plateau revealed by ice core tritium and mercury records. *Cryosphere*, **9**(3), 1213–1222 (doi: 10.5194/tc-9-1213-2015)
- Kargel JS, Leonard GJ, Bishop MP, Kääh A and Raup BH (2014) *Global land ice measurements from space*. Springer Berlin Heidelberg, Berlin, Heidelberg (doi: 10.1007/978-3-540-79818-7)
- Karnatak HC, Saran S, Bhatia K and Roy PS (2007) Multicriteria spatial decision analysis in web GIS environment. *Geoinformatica*, **11**(4), 407–429 (doi: 10.1007/s10707-006-0014-8)
- Kaspari S and 11 others (2007) Reduction in northward incursions of the South Asian monsoon since ~1400 AD inferred from a Mt. Everest ice core. *Geophys. Res. Lett.*, **34**(16), L16701 (doi: 10.1029/2007GL030440)
- Kaspari S and 7 others (2009a) A high-resolution record of atmospheric dust composition and variability since A.D. 1650 from a Mount Everest ice core. *J. Clim.*, **22**(14), 3910–3925 (doi: 10.1175/2009JCLI251.8.1)
- Kaspari S and 7 others (2009b) Recent increases in atmospheric concentrations of Bi, U, Cs, S and Ca from a 350-year Mount Everest ice core record. *J. Geophys. Res.*, **114**(D4), D04302 (doi: 10.1029/2008JD011088)
- Kawamura K and 17 others (2007) Northern Hemisphere forcing of climatic cycles in Antarctica over the past 360,000 years. *Nature*, **448**(7156), 912–916 (doi: 10.1038/nature06015)
- Kreutz KJ, Aizen VB, Cecil LD and Wake CP (2001) Oxygen isotopic and soluble ionic composition of a shallow firn core, Inilchek glacier, central Tien Shan. *J. Glaciol.*, **47**(159), 548–554 (doi: 10.3189/172756501781831819)
- Kumar P and 6 others (2015) Response of Karakoram-Himalayan glaciers to climate variability and climatic change: a regional climate model assessment. *Geophys. Res. Lett.*, **42**(6), 1818–1825 (doi: 10.1002/2015GL063392)
- Lee X, Qin D, Jiang G, Duan K and Zhou H (2003) Atmospheric pollution of a remote area of Tianshan Mountain: ice core record. *J. Geophys. Res.*, **108**(D14), 4406 (doi: 10.1029/2002JD002181)
- Lowell TV (2000) As climate changes, so do glaciers. *Proc. Natl. Acad. Sci. USA*, **97**(4), 1351–1354 (doi: 10.1073/pnas.97.4.1351)
- Mariani I and 6 others (2014) Temperature and precipitation signal in two Alpine ice cores over the period 1961–2001. *Clim. Past*, **10**(3), 1093–1108 (doi: 10.5194/cp-10-1093-2014)
- Mattavelli M and 6 others (2016) The IDB: an ice core geodatabase for paleoclimatic and glaciological analyses. *Geogr. Fis. Dinam. Quat.*, **39**(39), 59–70 (doi: 10.4461/GFDQ.2016.39.6)
- Mayer C and 6 others (2014) Accumulation studies at a high elevation glacier site in central Karakoram. *Adv. Meteorol.*, **2014**, 1–12 (doi: 10.1155/2014/215162)
- Mölg T, Maussion F and Scherer D (2013) Mid-latitude westerlies as a driver of glacier variability in monsoonal high Asia. *Nat. Clim. Change*, **4**(1), 68–73 (doi: 10.1038/nclimate2055)
- Müller WA and Roeckner E (2006) ENSO impact on midlatitude circulation patterns in future climate change projections. *Geophys. Res. Lett.*, **33**(5), L05711 (doi: 10.1029/2005GL025032)
- Neff PD and 5 others (2012) Ice-core net snow accumulation and seasonal snow chemistry at a temperate-glacier site: Mount Waddington, southwest British Columbia, Canada. *J. Glaciol.*, **58**(212), 1165–1175 (doi: 10.3189/2012JoG12J078)
- Orombelli G, Maggi V and Delmonte B (2010) Quaternary stratigraphy and ice cores. *Quat. Int.*, **219**(1), 55–65 (doi: 10.1016/j.quaint.2009.09.029)
- Papina T and 5 others (2013) Biological proxies recorded in a Belukha ice core, Russian Altai. *Clim. Past*, **9**(5), 2399–2411 (doi: 10.5194/cp-9-2399-2013)
- Petit JR and 18 others (1999) Climate and atmospheric history of the past 420,000 years from the Vostok ice core, Antarctica. *Nature*, **399**(6735), 429–436 (doi: 10.1038/20859)
- Pfeffer WT and 18 others (2014) The Randolph Glacier Inventory: a globally complete inventory of glaciers. *J. Glaciol.*, **60**(221), 537–552 (doi: 10.3189/2014JoG13J176)
- Pradhan B, Oh H-J and Buchroithner M (2010) Weights-of-evidence model applied to landslide susceptibility mapping in a tropical hilly area. *Geomatics, Nat. Hazards Risk*, **1**(3), 199–223 (doi: 10.1080/19475705.2010.498151)
- Preunkert S, Wagenbach D, Legrand M and Vincent C (2000) Col du Dome (Mt Blanc Massif, French Alps) suitability for ice-core studies in relation with past atmospheric chemistry over Europe. *Tellus, Ser. B Chem. Phys. Meteorol.*, **52**, 993–1012 (doi: 10.1034/j.1600-0889.2000.d01-8.x)
- Qu B and 8 others (2014) The decreasing albedo of the Zhadang glacier on western Nyainqentanglha and the role of light-absorbing impurities. *Atmos. Chem. Phys.*, **14**(20), 11117–11128 (doi: 10.5194/acp-14-11117-2014)
- Regmi NR, Giardino JR and Vitek JD (2010) Modeling susceptibility to landslides using the weight of evidence approach: western Colorado, USA. *Geomorphology*, **115**(1–2), 172–187 (doi: 10.1016/j.geomorph.2009.10.002)
- Schotterer U, Fröhlich K, Gäggeler HW, Sandjordj S and Stichler W (1997) Isotope records from Mongolian and alpine ice cores as climate indicators. *Clim. Change*, **36**(3/4), 519–530 (doi: 10.1023/A:1005338427567)
- Schotterer U, Stichler W and Ginot P (2004) The influence of post-depositional effects on ice core studies: examples from the Alps, Andes, and Altai. In Dewayne Cecil L, Green JR and Thompson LG, eds. *Earth paleoenvironments: records preserved in mid- and low-latitude glaciers*. Kluwer Academic Publishers, Dordrecht, 39–59 (doi: 10.1007/1-4020-2146-1_3)
- Schuster PF and 8 others (2002) Atmospheric mercury deposition during the last 270 years: a glacial ice core record of natural and anthropogenic sources. *Environ. Sci. Technol.*, **36**(11), 2303–2310 (doi: 10.1021/es0157503)
- Schwikowski M, Döschner A, Gäggeler HW and Schotterer U (1999) Anthropogenic versus natural sources of atmospheric sulphate from an Alpine ice core. *Tellus, Ser. B Chem. Phys. Meteorol.*, **51**, 938–951 (doi: 10.1034/j.1600-0889.1999.t01-4-00006.x)
- Schwikowski M and 11 others (2004) Post-17th-century changes of European lead emissions recorded in high-altitude alpine snow and ice. *Environ. Sci. Technol.*, **38**, 957–964 (doi: 10.1021/es034715o)
- Schwikowski M, Brüttsch S, Casassa G and Rivera A (2006) A potential high-elevation ice-core site at Hielo Patagónico Sur. *Ann. Glaciol.*, **43**(1995), 8–13 (doi: 10.3189/172756406781812014)
- Shekhar MS, Chand H, Kumar S, Srinivasan K and Ganju A (2010) Climate-change studies in the western Himalaya. *Ann. Glaciol.*, **51**(54), 105–112 (doi: 10.3189/172756410791386508)
- Singh RB and Mal S (2014) Trends and variability of monsoon and other rainfall seasons in Western Himalaya, India. *Atmos. Sci. Lett.*, **15**(3), 218–226 (doi: 10.1002/asl2.494)
- Sinha A and 7 others (2015) Trends and oscillations in the Indian summer monsoon rainfall over the last two millennia. *Nat. Commun.*, **6**, 6309 (doi: 10.1038/ncomms7309)
- Sterlacchini S, Ballabio C, Blahut J, Masetti M and Sorichetta A (2011) Spatial agreement of predicted patterns in landslide susceptibility maps. *Geomorphology*, **125**(1), 51–61 (doi: 10.1016/j.geomorph.2010.09.004)
- Svensson A and 13 others (2008) A 60 000 year Greenland stratigraphic ice core chronology. *Clim. Past*, **4**(1), 47–57 (doi: 10.5194/cp-4-47-2008)
- Tachikawa T and 11 others (2011) ASTER Global Digital Elevation Model Version 2 – summary of validation results. <https://pubs.er.usgs.gov/publication/70005960>
- Thevenon F, Anselmetti FS, Bernasconi SM and Schwikowski M (2009) Mineral dust and elemental black carbon records from an Alpine ice core (Colle Gnifetti glacier) over the last

- millennium. *J. Geophys. Res.*, **114**(D17), D17102 (doi: 10.1029/2008JD011490)
- Thiery Y, Malet JP, Sterlacchini S, Puissant A and Maquaire O (2007) Landslide susceptibility assessment by bivariate methods at large scales: application to a complex mountainous environment. *Geomorphology*, **92**(1–2), 38–59 (doi: 10.1016/j.geomorph.2007.02.020)
- Thompson LG (1996) Climatic changes for the 2000 years inferred from ice-core evidence in tropical ice cores. Jones PD, Bradley RS and Jouzel J eds. *Climatic variations and forcing mechanisms of the last 2000 years*. NATO ASI Series (Series I: Global Environmental Change). Springer, Berlin, Heidelberg, 281–295 (doi: 10.1007/978-3-642-61113-1_14)
- Thompson LG (2000) Ice core evidence for climate change in the Tropics: implications for our future. *Quat. Sci. Rev.*, **19**(1–5), 19–35 (doi: 10.1016/S0277-3791(99)00052-9)
- Thompson LG (2010) Understanding global climate change: paleoclimate perspective from the world's highest mountains. *Proc. Am. Philos. Soc.*, **154**(2), 133–157
- Thompson LG and 5 others (2000) A high-resolution millennial record of the South Asian Monsoon from Himalayan ice cores. *Science*, **289**(5486), 1916–1919 (doi: 10.1126/science.289.5486.1916)
- Thompson LG and 5 others (2003) Tropical glacier and ice core evidence of climate change on annual to millennial time scales. *Clim. Change*, **59**, 137–155 (doi: 10.1023/A:1024472313775)
- Thompson LG and 5 others (2005) Tropical ice core records: evidence for asynchronous glaciation on Milankovitch timescales. *J. Quat. Sci.*, **20**, 723–733 (doi: 10.1002/jqs.972)
- Thompson LG, Mosley-Thompson E, Davis ME and Brecher HH (2011) Tropical glaciers, recorders and indicators of climate change, are disappearing globally. *Ann. Glaciol.*, **52**(59), 23–34 (doi: 10.3189/172756411799096231)
- Thompson LG and 6 others (2013) Annually resolved ice core records of tropical climate variability over the past 1800 years. *Science*, **340**(6135), 945–950 (doi: 10.1126/science.1234210)
- Tian L and 7 others (2003) Oxygen-18 concentrations in recent precipitation and ice cores on the Tibetan Plateau. *J. Geophys. Res.*, **108**(D9), 1–10 (doi: 10.1029/2002JD002173)
- Vimeux F and 6 others (2009) Climate variability during the last 1000 years inferred from Andean ice cores: a review of methodology and recent results. *Palaeogeogr. Palaeoclimatol. Palaeoecol.*, **281**(3–4), 229–241 (doi: 10.1016/j.palaeo.2008.03.054)
- Vincent C and 6 others (2005) Glacier fluctuations in the Alps and in the tropical Andes. *C. R. Geosci.*, **337**(1–2), 97–106 (doi: 10.1016/j.crte.2004.08.010)
- Wagenbach D and Geis K (1989) The mineral dust record in a high altitude alpine glacier (Colle Gnifetti, Swiss Alps). In Leinen M and Sarnthein M, eds. *Paleoclimatology and paleometeorology: modern and past patterns of global atmospheric transport*. Kluwer Academic Publishers, London, 543–564 (doi: 10.1017/CBO9781107415324.004)
- Wagenbach D, Bohleber P and Preunkert S (2012) Cold, alpine ice bodies revisited: what may we learn from their impurity and isotope content? *Geogr. Ann. Ser. A Phys. Geogr.*, **94**(2), 245–263 (doi: 10.1111/j.1468-0459.2012.00461.x)
- Wake CP (1989) Glaciochemical investigations as a tool for determining the spatial and seasonal variation of snow accumulation in the central Karakoram, northern Pakistan. *Ann. Glaciol.*, **13**, 279–284
- Welch BC, Pfeffer WT, Harper JT and Humphrey NF (1998) Mapping subglacial surfaces of temperate valley glaciers by two-pass migration of a radio-echo sounding survey. *J. Glaciol.*, **44**(146), 164–170
- Whan K and Zwiers F (2017) The impact of ENSO and the NAO on extreme winter precipitation in North America in observations and regional climate models. *Clim. Dyn.*, **48**(5), 1401–1411 (doi: 10.1007/s00382-016-3148-x)
- Wilson JP and Gallant JC (2000) *Terrain analysis: principles and applications*. John Wiley & Sons Inc. (doi: 0471321885)
- Xu B and 11 others (2009) Black soot and the survival of Tibetan glaciers. *Proc. Natl. Acad. Sci.*, **106**(52), 22114–22118 (doi: 10.1073/pnas.0910444106)
- Yang X, Joswiak D and Yao P (2014) Integration of Tibetan Plateau ice-core temperature records and the influence of atmospheric circulation on isotopic signals in the past century. *Quat. Res.*, **81**(3), 520–530 (doi: 10.1016/j.yqres.2014.01.006)
- Yao T and 14 others (2012) Different glacier status with atmospheric circulations in Tibetan Plateau and surroundings. *Nat. Clim. Change*, **2**(9), 663–667 (doi: 10.1038/nclimate1580)
- Ye D-Z and Wu G-X (1998) The role of the heat source of the Tibetan Plateau in the general circulation. *Meteorol. Atmos. Phys.*, **67**(1–4), 181–198 (doi: 10.1007/BF01277509)
- Yu W and 10 others (2016) $\Delta 18\text{o}$ records in water vapor and an ice core from the eastern Pamir Plateau: implications for paleoclimate reconstructions. *Earth Planet. Sci. Lett.*, **456**, 146–156 (doi: 10.1016/j.epsl.2016.10.001)
- Zhang Q, Kang S, Gabrielli P, Loewen M and Schwikowski M (2015) Vanishing high mountain glacial archives: challenges and perspectives. *Environ. Sci. Technol.*, **49**(16), 9499–9500 (doi: 10.1021/acs.est.5b03066)
- Zhao H, Xu B, Yao T, Tian L and Li Z (2011) Records of sulfate and nitrate in an ice core from Mount Muztagata, Central Asia. *J. Geophys. Res.*, **116**(D13), D13304 (doi: 10.1029/2011JD015735)
- Zhisheng A, Kutzbach JE, Prell WL and Porter SC (2001) Evolution of Asian monsoons and phased uplift of the Himalaya-Tibetan plateau since late Miocene times. *Nature*, **411**(6833), 62–66 (doi: 10.1038/35075035)

MS received 18 September 2017 and accepted in revised form 18 October 2017; first published online 11 December 2017